iScience

CellPress
OPEN ACCESS

Review

Recent advances in computational design of structural multi-principal element alloys

Abu Anand,[1] Szu-Jia Liu,[1] and Chandra Veer Singh[1,2,*]

SUMMARY

Multi-principal element alloys (MPEAs) have gained extensive interest for structural applications owing to their excellent strength, fracture toughness, wear resistance, creep resistance, and fatigue resistance. In this review, recent progress in the computational design of MPEAs for structural applications is outlined. This includes the scientific advancements achieved through computational methods in the field of structural MPEAs, how new methodologies have emerged due to the needs of complex alloy systems, and adaptations to the existing tools to address emerging problems in the field. We discuss advances in atomistic simulation methods, including structure generation algorithms, element-resolved local lattice distortion, chemical short-range order, local slip resistance, and radiation tolerance, along with experimental comparisons. A detailed discussion on interatomic potentials is included, with a focus on various machine learning-based fitting methods. The application of data science and machine learning for identifying and discovering MPEAs with desirable mechanical performance is summarized and presented.

INTRODUCTION

Traditionally, alloy design relies on the selection of one or two principal elements and small amounts of alloying elements to attain the desired properties. On the contrary, multi-principal element alloys (MPEAs), introduced nearly two decades ago, are mixtures of multiple principal components. The unique properties of MPEAs are attributed to the improved stability of solid solution phases, including body-centered cubic (BCC), face-centered cubic (FCC), and hexagonal close-packed (HCP), achieved by maximizing the configurational entropy as the number of constitutional elements increases.[1,2]

The exceptional mechanical properties of MPEAs are of great significance for structural applications. The BCC-structured refractory HfNbTaTiZr alloy reaches a tensile strength of 1,262 MPa while maintaining a ductility of 9.7% after annealing at 1,000°C.[3–5] The equiatomic CoCrFeMnNi alloy forms a single-phase FCC solid solution and possesses superior tensile strength of 1,280 GPa and fracture toughness of 200 MPa $m^{1/2}$ at cryogenic temperatures.[6–8] MPEAs have also demonstrated excellent wear resistance, creep resistance, and fatigue resistance. CoCrMoxNi showed improved wear resistance with increasing concentration of Mo, stabilizing with $x > 0.5$.[9–11] In addition, nanocrystalline CoCrFeMnNi displays improved creep resistance than conventional nanocrystalline Ni due to sluggish diffusion.[7,8,12,13] Furthermore, the $Al_{0.5}$CoCrCuFeNi MPEA revealed promising fatigue resistance surpassing conventional alloy counterparts.[14–16]

Although the experimental process is still the most popular approach when it comes to alloy design, it is often time-consuming and laborious, considering the vast compositional space of MPEAs. On the other hand, the computational method has been attracting more attention in recent years due to its "high throughput" nature and parametric control. Computational design and MPEA research have had a reciprocal relationship since the discovery of MPEAs, both mutually benefiting the other. Discovery and development of MPEAs called for revisiting every fundamental aspect of alloys from the perspective of concentrated solid solutions. While computational methods have a vital role in this process, MPEAs came with their challenges, apropos to their configurational and compositional complexity, to directly use the conventional computational methods. Over the years, this has led to a constant call for adapting these methods and using them to understand MPEAs. In this review, we aim to present recent developments on how new computational techniques are developed or how the existing ones are adapted for structural MPEA design, and the advancements these methods have brought forth in the field. We primarily focus on atomistic methods, potential energy surface (PES) fitting, data science- and machine learning (ML)-based methods, and how these are used in tandem to develop new structural MPEAs.

ATOMISTIC CALCULATIONS

A wide compositional space has presented promises and challenges in the field of MPEAs. Conventional trial-and-error methods, although effective for classical alloys, have proven to be rather inefficient when it comes to the MPEA paradigm. Atomistic methods can be used as a

[1]Department of Materials Science and Engineering, University of Toronto, 184 College Street, Toronto, ON M5S 3E4, Canada
[2]Department of Mechanical and Industrial Engineering, University of Toronto, 5 King's College Road, Toronto, ON M5S 3G8, Canada
*Correspondence: chandraveer.singh@utoronto.ca
https://doi.org/10.1016/j.isci.2023.107751

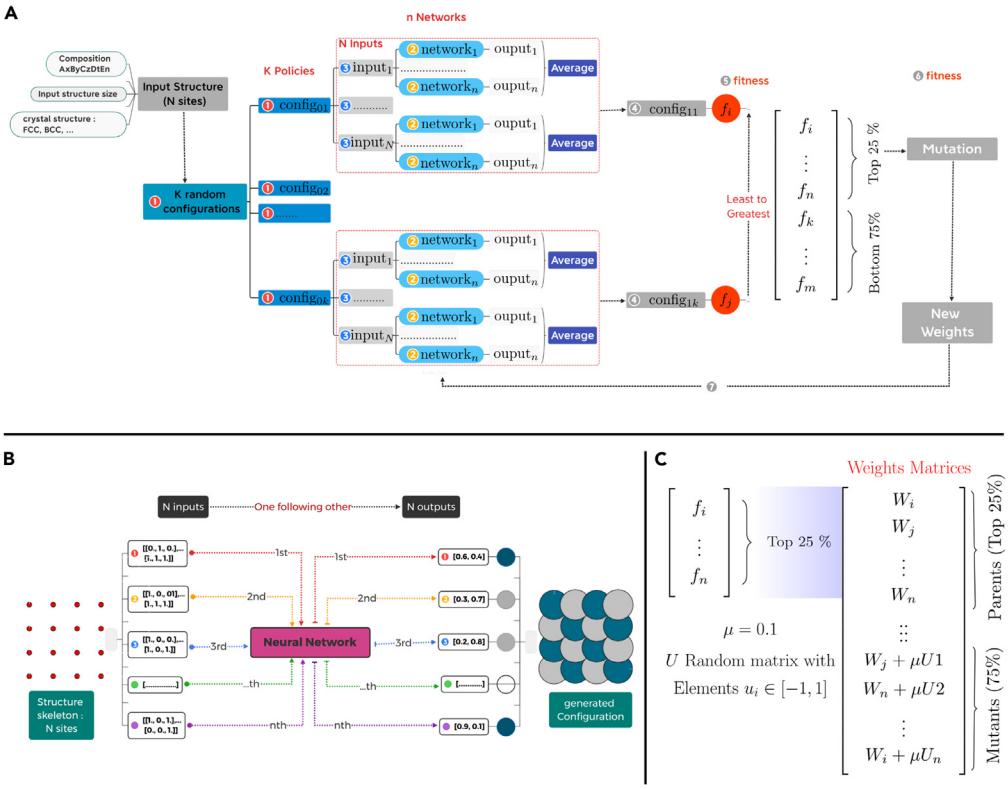

Figure 1. A sketch of the required algorithms for the NES training process

(A) NES training process (B) NES generation process (C) Outline of the mutation step. Reprinted from[21] with the permission of AIP publishing.

powerful alternative to guide the development of new compositions. In this section, we explore the advances that have been made in recent years through various atomistic simulation techniques in the design of MPEAs.

Atomistic structure generation

Generating reliable structures to simulate MPEAs has always been a challenge. The special quasi-random structures (SQSs) method has been widely adopted to generate supercells for atomistic simulations. Various methods to generate SQSs have been implemented through Monte Carlo and cluster expansion algorithms,[17–20] although reliable, SQS generation is computationally intensive and scales poorly as the number of atoms in the system increases. This has shown to be a bottleneck in generating reliable MPEA structures for simulations that require relatively large representative supercells especially when it comes to large-scale classical simulations. Conventional alloy systems usually do not encounter this challenge because of their dilute compositions leading to a lower degree of randomness in the lattice. A need for reliable MPEA structure generation has led to the development of new algorithms. Neural evolution structure (NES) generator combines evolutionary algorithms with artificial neural networks (ANNs) to generate MPEA structures.[21] Figure 1 illustrates the workflow for NES structure generation outlining the NES training process and generation process. Here an ANN is trained using a smaller system, and a larger system is generated using this trained model. Compared to the SQS approach, NES can bring down the computational complexity of structure generation dramatically and has been utilized to create structures with over 40,000 atoms at a reasonable computational overhead (a few hours on 40 processors).

Short-range order (SRO) is a key aspect to consider while performing atomistic and mesoscale simulations for MPEAs. Introducing SRO into these systems often involves performing computationally intensive Monte Carlo simulations. As an alternative, a statistical smart swapping procedure named order through informed swapping (OTIS) has been introduced to create lattices with given SRO parameters from an initial random lattice. This method can be used to create a system with hundreds of thousands of atoms.[22] A combination of NES[21] and OTIS[22] methods can be used to create MPEA structures that could be used in large-scale atomistic simulations.

Density functional theory (DFT)

DFT has been extensively used to simulate MPEAs. As it does not rely on any empirical data or models, DFT can significantly support the exploration of the elemental while requiring minimal adaptations to conventional tools. In this section, we explore the recent advancements made in structural MPEA research utilizing DFT.

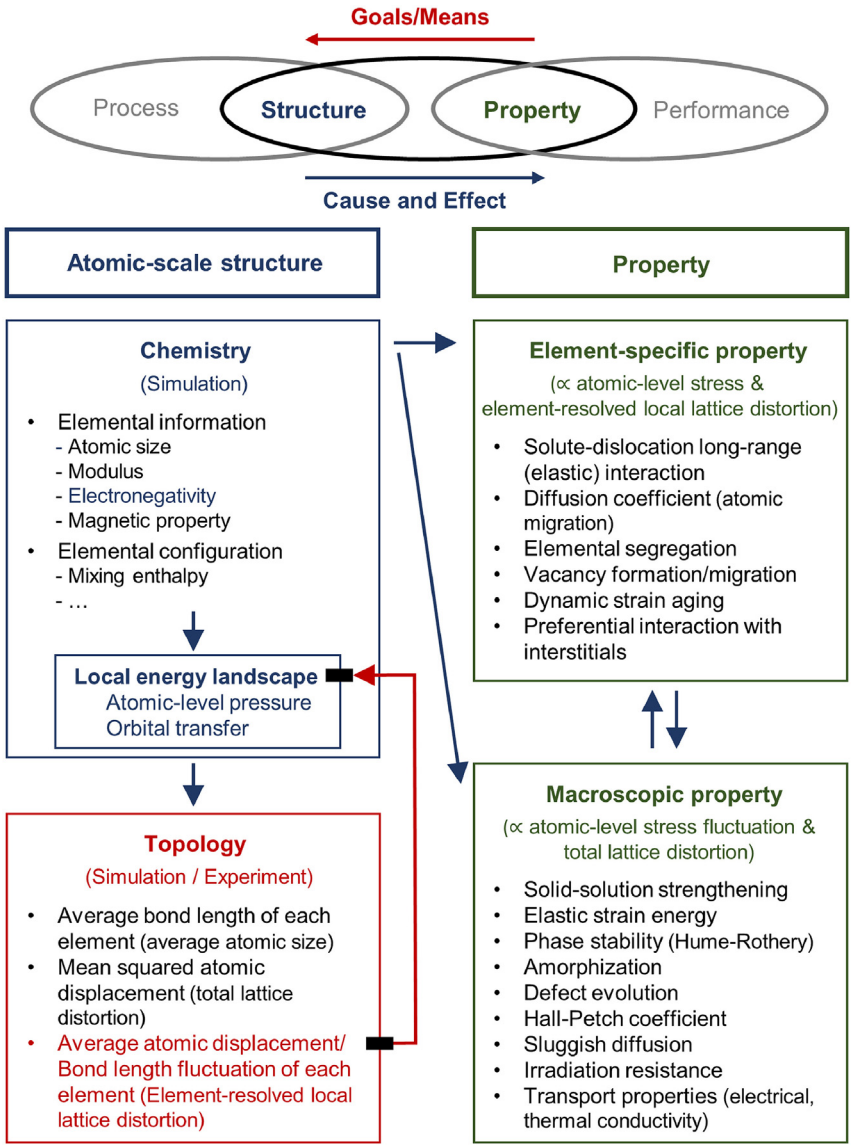

Figure 2. System chart for MPEA atomic-scale design route

Cause-and-effect logic of science is indicated by the blue arrow. The red arrow indicates the goal-means relations of the engineering flow,[23] reprinted with permission from Elsevier.

Severe lattice distortion has been in the spotlight for a multitude of properties in complex alloys, including but not limited to solid-solution strengthening, irradiation resistance, and sluggish diffusion.[23–25] The lack of local symmetry results in lattice distortion fields accessible through *ab initio* calculations. These local lattice distortion (LLD) fields have been correlated with experimentally measured yield strengths.[26,27] It has been shown that for single-phase FCC MPEA solid solutions, lattice distortions improve the friction stress and thus elevate the strength and its sensitivity toward grain size.[28] Charge transfer between the constituent elements dictates the element-resolved local lattice distortion (ELLD) in the complex alloys of 3d transition metals.[29] This affects the properties of the alloy through atomic pressure and orbital transition. ELLD is presented as an observable signature of charge transfer which can be used to develop an understanding of how the local atomic structure will affect the structural properties of MPEAs. Figure 2 shows the relationship between atomic structure and properties of the 3d transition metal complex alloys. The properties are divided into two groups—element-specific set that can be related to ELLD and macroscopic properties that are suggested to be proportional to the total lattice distortion.

Determining chemical SRO in MPEA systems has extensively relied on DFT-based techniques. Recently, concentration wave analysis in conjunction with DFT and linear response theory has been used to determine the phase stability of Ti0.25CrFeNiAlx system.[30] This approach can be extended to any arbitrary MPEA system to assess the possible low-temperature competing partially ordered states. Chemical SRO in

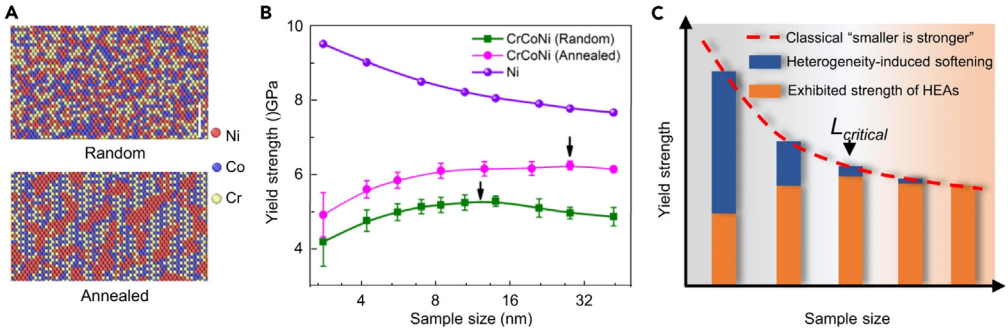

Figure 3. Size-dependent yield strength of CrCoNi MPEA using MD simulations

(A) Showing the random solid solution and the annealed structure with local segregations.

(B) Variation of yield strength for both random and annealed structures as a function of sample size (C) size effect in MPEAs.[40]

TiZrHfNb results in the favoring of Ti-Zr and Nb-Hf neighbor pairs in line with the previous experimental results.[31] A vacancy atom SRO is suppressing atomic SRO in equiatomic TiZrHfAl, which in turn selects a γ-brass-like BCC superstructure with four vacancies per cell.[32]

While *ab initio* methods are of paramount importance to the basic property calculations of MPEAs, size and timescale limitations cannot be overlooked. For structural applications, accurate calculation of ductility and strength is critical. However, this requires capturing the motion and interactions of dislocations in the complex MPEA system. It is challenging for the current *ab initio* methods to get to this size and time-scale, even for elemental systems. A theoretical model has been developed utilizing data from first-principle calculations to predict the yield strength in RhIrPdPtNiCu high-entropy alloy.[33] This model utilizes solute misfit volumes, alloy lattice constants, elastic constants, and stable stacking fault energies to predict the strength of the alloy. As these properties are accessible through DFT calculations, this model connects a complex alloy composition to the yield strength without any experimental inputs.

Classical molecular dynamics (MD)

Classical MD simulations have been applied to provide critical insights into the structural properties of MPEAs. Compared to DFT-based methods, classical MD can simulate larger system sizes and can be used to explore various time and temperature-dependent phenomena efficiently. Thus, it has been critical in the computational research of structural MPEAs to efficiently utilize classical MD to its full capability. While most of the conventional tools can be translated to MPEAs without significant overhead, these simulations require a defined PES through an interatomic potential (IP) to carry out simulations. This has proven to be a major challenge in using classical MD in MPEA research. There have been classical and ML-based interatomic potentials (ML-IPs) developed for MPEA systems which will be discussed in this section along with key scientific advances enabled by classical MD in the field of these complex alloy systems.

Plasticity mechanisms and dislocation dynamics in MPEAs have been investigated using classical MD. Chen et al. showed that the compositional inhomogeneities in a BCC MPEA make kink nucleation the rate-limiting mechanism for dislocation mobility.[34] Contrary to classical BCC alloys, the edge dislocations also encounter a comparable activation barrier as the screw dislocations due to nanoscale segment trapping. This results in an equal contribution of edge and screw dislocations toward the strength of the alloy.[34] Similar to Peierls stress, a local slip resistance (LSR) can be defined in an MPEA, which accounts for any local solute environment encountered by a dislocation as it moves through the alloy.[35] Transmission electron microscopy (TEM) evidence shows that in BCC MoNbTi, dislocations can glide on higher-order planes. Molecular statistics calculations show that the variation of chemical species affects LSR significantly for the dislocations on the same type of slip plane.[36] LSR and lattice distortion were found to be positively correlated, while the anisotropy in LSR was reduced with lattice distortion. Cr-containing MPEAs have larger lattice distortion compared to the non-Cr-containing counterparts.[37] Compositional heterogeneities and local chemical environments impact the mechanical properties of MPEAs.[38–40] Yan J. et al. reported MD simulations correlated with experimental results showing the impact of local elemental segregations on the yield strength of CrCoNi MPEA (Figure 3).[40]

MPEAs have been shown to have enhanced radiation tolerance.[41–44] SRO can be induced because of ion irradiation resulting from biased elemental diffusion. A higher defect recombination rate has been observed in the NiCoCrFe system compared to elemental Ni.[45,46] This is induced by enhanced thermal spike, lower thermal conductivity, and smaller binding energy of interstitials, which affects the cascade evolution and suppresses the damage accumulation.[46,47] Nickel segregation happens at the early stages of radiation damage in Co-, Fe-, Cr-, and Ni-containing systems.[48] Stacking fault tetrahedra (SFTs) are expected to form in FCC MPEAs during irradiation damage. Earlier, this was not observed experimentally or in atomistic simulations and was attributed to the negative values for the binding energies of tri-vacancy clusters.[49–51] Recently, a combination of classical MD simulations with scanning transmission electron microscopy (STEM) imaging identified SFTs in CoCrNi medium entropy alloy.[52] It should be noted that the tetra-vacancy clusters have a positive binding energy in CoCrFeMnNi, suggesting that these vacancy clusters can form when cascade damage is caused by high-energy ion or neutron irradiation.[49]

ML-IPs trained using first-principles data are widely utilized to model PESs of various systems. This allows one to efficiently bridge the gap between *ab initio* simulations and classical MD and to access more extensive time and size scales. Classical MD simulations on MPEAs were carried out using semi-empirical embedded atom method (EAM) potentials in the initial years.[46,53,54] Although effective, classical potentials

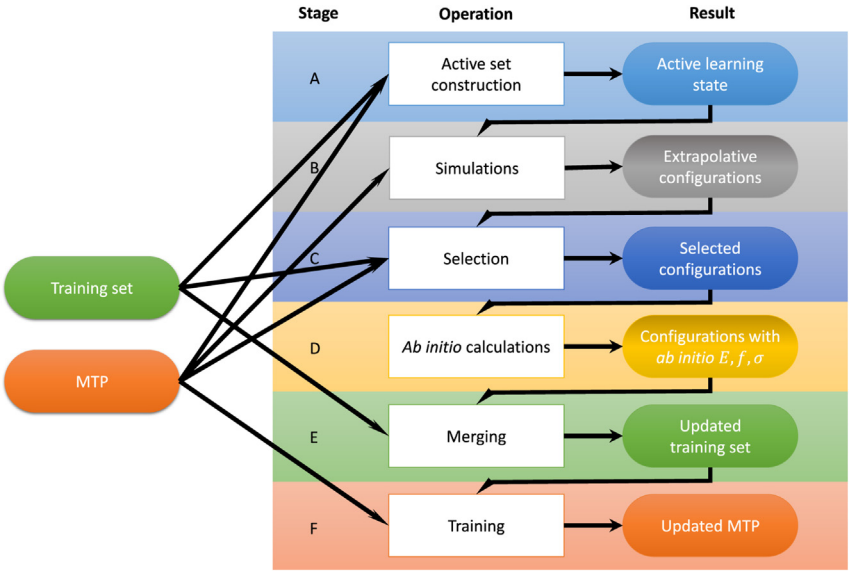

Figure 4. Schematic of a single iteration of the active learning algorithm for the on-the-fly approach of training an MTP potential
Reprinted from Novikov et al (under CC BY 4.0).[59]

are limited in their functional forms and miss out on complex chemical interactions in MPEA systems. ML-IPs have been extensively used to simulate MPEAs in recent years.

Moment tensor potentials (MTPs) are a set of ML-IPs which describe the local atomic environment of an atom of interest by the moment of inertia of the neighboring atoms.[55] This class of potentials has been shown to outperform other ML-IPs and classical potentials.[56,57] On-the-fly trained MTPs are used to simulate MPEAs.[58] On-the-fly learning is an active learning approach that can significantly speed up the atomistic simulation process and enable high-throughput calculations. A single iteration of the active learning algorithm is shown in Figure 4.[59] LLD, discussed in a previous section, was studied in the CoFeNi system using an MTP. It was shown that the probability distribution of LLDs affects the structural properties of MPEAs.[58] The effect of SRO in the dislocation mobility of NbMoTaW was shown using an MTP.[60] Thermodynamic integration aided by MTP was introduced recently to accurately and efficiently simulate the high-temperature properties of MPEAs.[61] This approach offers a four-times speedup compared to the DFT-based approaches while having a less than 1 meV/atom error on the high-temperature free energy predictions.

Low-rank potentials (LRPs) are specifically suited for multi-component alloys utilizing an on-lattice method. Proposed as an alternative to cluster expansion methods which are not effective in handling multi-component systems, LRPs only have two adjustable parameters: the range of the interatomic interaction and the upper bound on the tensor rank where the latter controls the number of free parameters in the model.[62] LRP-based computational approach considering local atomic relaxations found that the NbMoTaW solid solution transforms into a layered semiordered metastable phase.[63] Formation of iron and chromium sublattices at temperatures below 600°C and 1,230°C, respectively, was observed in CoCrFeNi FCC alloy through an on-lattice Metropolis Monte Carlo algorithm using an LRP.[64]

Kernel-based models such as Gaussian approximation potential (GAP) have been proposed to fit IPs,[65] although this will be inefficient with MPEAs as the number of three-body and two-body interactions can scale significantly with the number of component elements. A potential based on generalized linear models has been proposed recently for FeNiCuCoCr FCC MPEA. The random Fourier feature (RFF)-based IP has shown accurately the mechanical and thermal properties of the MPEA system close to the DFT calculated values. Further, a sparse Bayesian learning-based potential has been proposed to reduce the computational overhead of the RFF potential by 94%.[66,67]

SRO and strengthening mechanisms in NbMoTaW refractory High Entropy Alloy (HEA) system were studied using a spectral neighbor analysis potential (SNAP).[68,69] An SNAP model expresses the energies and forces from the *ab initio* data as a function of coefficients of the bispectrum of the atomic neighbor density function.[70] A high-level workflow of the SNAP potential fitting is illustrated in Figure 5. Fitted to the DFT data of elemental, binary, ternary, and quaternary combinations of the component elements, this potential demonstrated that the strengthening in the NbMoTaW alloy is due to the segregation of Nb to the grain boundaries leading to SRO.[68]

DATA SCIENCE AND MACHINE LEARNING

The design of MPEAs has primarily relied on a trial-and-error approach, but compared to conventional alloys, the search space for MPEAs is considerably vast. The number of unique combinations of MPEA systems composed of 40 metallic elements can be estimated by $C_r^n = \frac{n!}{r!(n-r)!}$. There are potentially 9,880 three-component, 91,390 four-component, 658,008 five-component, 3,838,380 six-component, and 18,643,560 seven-component alloy systems. In other words, they can form 23,241,218 distinct equiatomic MPEAs. Furthermore, by varying

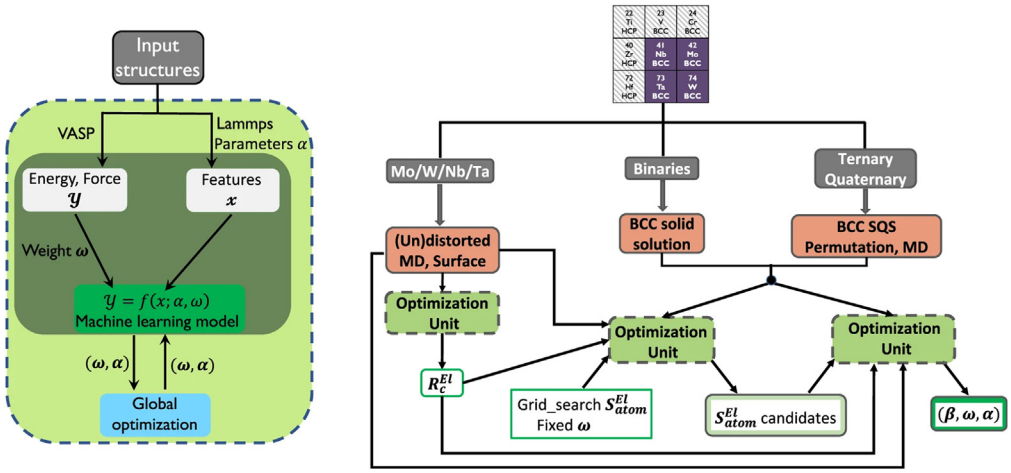

Figure 5. Fitting workflow schematic for the NbMoTaW alloy SNAP model
Reprinted from Li et al (under CC BY 4.0).[68]

the elemental compositions, the number of base alloys that can be formed is enormous, and it is laborious and impractical to manually explore the entire collection MPEAs and study their microstructures, phases, and mechanical properties.

The emergence of ML, on the other hand, offers a novel breakthrough point for MPEA exploration. Among the three major categories of ML, supervised learning, unsupervised learning, and reinforcement learning, supervised learning is extensively applied in materials science. It facilitates the derivation of relationships between the input and output properties, seeking explanations of what leads to the desired properties of certain materials and how one can enhance their performance even further. Essentially, material scientists are always pursuing materials with extraordinary properties. Thus, in the interest of high-throughput material design, the successful extrapolation of existing data becomes paramount when adapting ML in the design process.

In ML-assisted material design, there are typically four main aspects one should consider, namely, the targeted output properties, the construction of material databases, the selection of descriptors, and the development of ML models, all of which will be reviewed in subsequent sections. Table 1 gives a summary of some of the recently published works from the aforementioned aspects.

The objective of the ML task would be the first and foremost consideration because the three remaining steps are based on the targeted outcome. In terms of the design of structural MPEAs, one of the applications is phase selection, where the ML model is designed to predict whether the MPEAs are in BCC, FCC, or HCP phase and if intermetallic (IM) or amorphous phases are present.[71–73] One hundred fifty ANNs were trained using an experimental MPEA dataset with 323 data points to predict the occurrence of phases present in the alloys that were categorized into seven classes, including the formation of FCC, BCC, intermetallics, or combinations of them.[72] Later, a reduced mathematical model was developed to classify the presence and absence of BCC and FCC phases within a 13-element search space for MPEAs.[73] The model was reported to have comparable performance to neural network models, having high interpretability at the same time. Other usages include the prediction of various mechanical properties, such as elastic constants,[74–76] hardness,[77,78] yield strength,[79,80] and Young's modulus.[80–82] A recent study combined DFT and ML to explore the optimal compositional space of the non-equiatomic MoNbTaTiV system using the element composition as the only feature and identified Ti as the critical factor that could potentially compromise Young's modulus of the MPEA.[82]

The performance of ML work is heavily dependent on the quality of data. In the field of MPEAs, datasets generally come from two categories, experimental and computational. Experimental databases contain measurements using various characterization techniques. In contrast, computational databases are developed using DFT calculations, MD simulations, and the CALculation of PHAse Diagrams (CALPHAD) method. While a large amount of experimental data are readily available for MPEAs, there are usually discrepancies between the reported values due to different fabrication and post-processing methods. For instance, the yield strength reported for CoCrFeMnNi processed with cold rolling and annealing varies significantly from 380 to 1,210 MPa.[83–85] To mitigate the potential variations arising from different material preparation conditions, a common approach is to select data of which the materials are prepared similarly. Examples include the phase prediction study by Beniwal et al.,[72] where the dataset is all taken from 323 as-cast MPEAs tested at room temperature. Another strategy is to compare across literature values and use the average of those that do not differ significantly, as demonstrated by Wen et al.[77] Nonetheless, computational approaches tend to show a preferred consistency across the calculated values, but constructing a large computational database across different elements is quite computationally expensive. In addition, specific mechanical properties, such as yield strength, are challenging to obtain owing to the limited availability of IP files for MPEAs. Recently, a theoretical method proposed by Yin et al.[33] is capable of predicting yield strength using DFT data. Such an approach can be a potential solution for overcoming the limitation of computational databases.

Despite the increasing research efforts in the field, only a limited number of well-structured databases exist for MPEAs. Thermodynamics data for 355 MPEA compositions, combining empirical and theoretical approaches using the Hume-Rothery rules, were published by Gao

Table 1. Recent studies on data-driven MPEA design along with output properties, material database, descriptors (defined in Table S1 in supplemental information), best-performing ML algorithms, and model outcome

Reference	Output properties	Material database	Descriptors	Best-performing ML algorithms	Model outcome
Pei et al.[71]	Phases: single-phase, multi-phase	1252 binary and MPEA systems (625 single-phase and 627 multi-phase, empirical)	V_m, K, χ, T_m, VEC, ΔH_{vap}	Classification: Gaussian process classification (GPC)	Accuracy: 93% with GPC; 81% with empirical rule
Beniwal et al.[72]	Phases: FCC, BCC, FCC+BCC, FCC+IM, BCC+IM, FCC+BCC +IM, IM	323 MPEAs (empirical)	δV_m, δR_{met}, ΔS_{config}, δR_{cov}, E_{coh}, δE_{coh}, δK, δE, δG, VEC, χ^{Allen}, ρ, ΔH^{el}, $\Delta H_{SS}^{chem}(L)$	Classification: artificial neural network (ANN)	Accuracy: 84%
Beniwal et al.[73]	Phases: BCC, FCC, BCC+FCC, neither BCC nor FCC	426 MPEAs (empirical)	VEC, δR_{met}, δR_{cov}, δE, E_{coh}, $\Delta H_{SS}^{chem}(L)$, ΔH^{el}	Classification: neural network (NN)	Accuracy: 91% (BCC), 95% (FCC)
Revi et al.[74]	Elastic constants: C_{11}, C_{22}, C_{33}, C_{12}, C_{13}, C_{23}, C_{44}, C_{55}, C_{66}	1229 binary alloys from Materials Project (DFT)	a_0, ρ, VEC, T_m, k	Regression: random forest (RF)	RMSE: 34.61 GPa, MAE: 23.46 GPa, R^2: 0.779
Bhandari et al.[75]	Elastic constants: C_{11}, C_{12}, C_{44}	370 MPEAs (DFT)	ΔS_{config}, ΔH, T_m, Ω, δr, VEC, $\delta\chi$, λ, name of alloys	Regression: gradient boosting regressor (GBR)	RMSE: 12.68 GPa, MAE: 9.62 GPa, R^2: 0.853
Vazquez et al.[76]	Elastic constants: C_{11}, C_{12}, C_{44}	110 binary and 60 ternary systems (DFT)	$\overline{Z}$, $\overline{P}$, a_0, χ, χ^{Allen}, ρ, ΔH^{form}, a, T_m, E_a, VEC	Regression: sure independence screening and sparsifying operator (SISSO)	RMSE: 8.69 GPa, R^2: 0.948
Wen et al.[77]	Hardness	22 quaternary, 95 quinary, and 38 senary systems (empirical)	e/a, w, η	Regression: support vector regression with radial basis function kernel (svr.r)	Found $Al_{47}Co_{20}Cr_{18}Cu_5Fe_5Ni_5$ with 883 HV, 14% higher than the best value in the original dataset
Yang et al.[78]	Hardness	36 quaternary, 178 quinary, 132 senary, and 24 septenary systems (empirical)	$\hat{u}$, $\hat{C}$, $\hat{v}$, VEC, T_m	Regression: support vector regression with radial basis function kernel (svr.r)	Found $Co_{18}Cr_7Fe_{35}Ni_5V_{35}$ with 920 HV, 25% higher than the best value in the original dataset
Zhang et al.[79]	Yield strength: good and weak compared to the equiatomic sample	300 single-crystal CoCrFeMnNi samples (MD)	Element composition	Classification: deep neural network (DNN)	F1-Score: 94.3%

(*Continued on next page*)

Table 1. *Continued*

Reference	Output properties	Material database	Descriptors	Best-performing ML algorithms	Model outcome
Zhang et al.[80]	Yield strength, Young's modulus	900 single-crystal CoCrCuFeNi samples (MD)	Element composition	Regression: kernel-based extreme learning machine (KELM)	F1-Score: 88.1% (Yield strength) F1-Score: 92.9% (Young's modulus)
Khakurel et al.[81]	Young's modulus	154 refractory and non-refractory MPEAs (empirical); 96 refractory binary and MPEA systems (empirical)	$\delta\chi$, ΔH, ΔS_{config}, δa, δT_m, λ, Ω, T_m, a, VEC	Regression: gradient boosting (GB)	MAE: 10.37 GPa, R^2: 0.71 (refractory and non-refractory) MAE: 6.15 GPa, R^2: 0.90 (refractory)
Gao et al.[82]	Young's modulus	200 MoNbTaTiV samples (DFT)	Element composition	Regression: eXtreme Gradient Boosting (XGBoost)	RMSE: 4.28 GPa, MAE: 3.47 GPa, R^2: 0.92

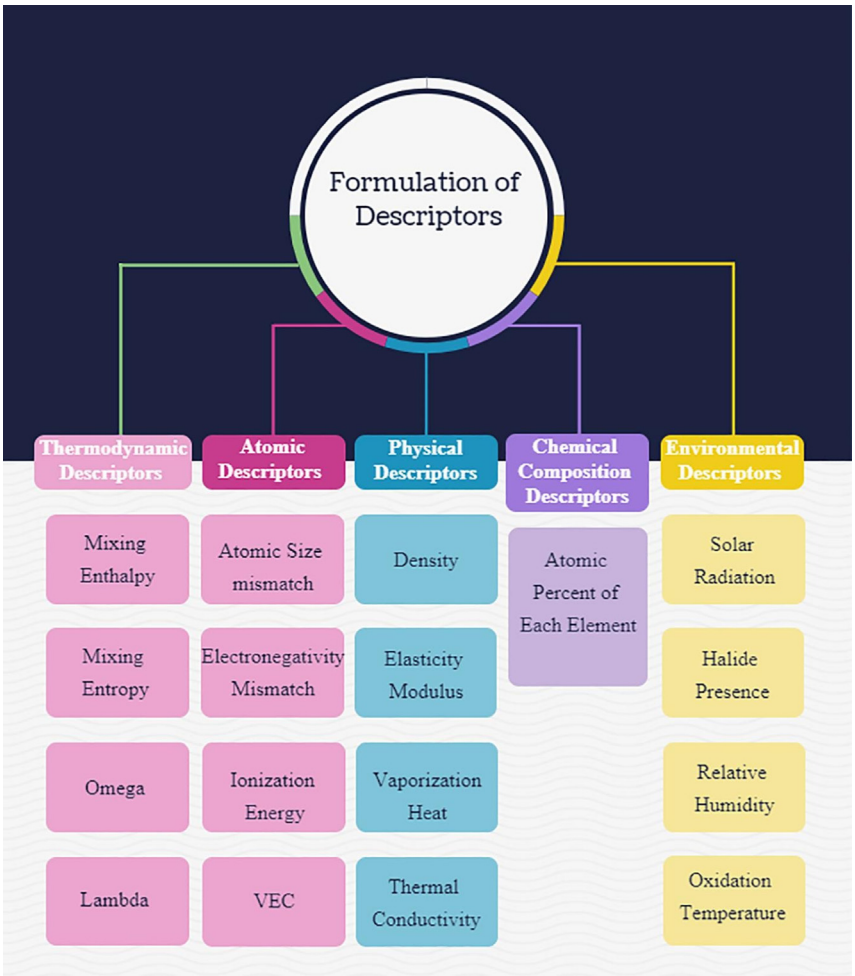

Figure 6. The typical categorization of MPEA descriptors together with select examples
Reprinted with permission from Elsevier.[90]

et al.[86] In a subsequent review, Borg et al.[87] compiled and updated a database based on two previous reviews of MPEAs,[88,89] incorporating phases and mechanical properties of 630 MPEAs from 265 articles containing experimentally measured yield strength, ultimate tensile strength, hardness, and elongation. However, there is a lack of consistency in the reported properties, and a more comprehensive database needs to be adopted by ML-assisted MPEA design.

An ideal ML model takes only the compositions of the MPEA systems and makes predictions about the desired properties. However, using elemental compositions solely is typically insufficient for adequate model performance, and other descriptors are required. In an ML study on MPEAs, Roy et al.[90] classified a list of 94 features employed into five categories: atomic, chemical composition, environmental, physical, and thermodynamic, and some examples from each category are illustrated in Figure 6.

The descriptors employed in the ML models are determined by the properties to be predicted. Some commonly accepted features for phase selection include the difference in atomic radii, the difference in electronegativities, mixing enthalpy, mixing entropy, and valence electron concentration.[91–96] Moreover, King et al.[97] introduced a novel parameter that suggests a value of $\Phi \geq 1$, where $\Phi = \frac{\Delta G_{ss}}{-|\Delta G_{max}|}$, indicates the formation of a stable solid solution phase at the melting point. A newly published ML work conducted by Zhao et al.[96] provides additional evidence for this observation. On the contrary, for predicting mechanical properties, in addition to the above five features, a variety of other predictors are also taken into account depending on the ML models and the feature selection methods applied. For instance, Wen et al.[77] investigated the performance of the ML model with different subsets of twenty preselected features and found that three features, namely, the number of itinerant electrons, the sixth square of the work function, and modulus mismatch, simplified the model without jeopardizing the accuracy of hardness prediction. Another work by Yang et al.[78] considered 142 features and after four screening stages selected five key features, including the average deviations of atomic weight, column and specific volume, as well as valence electron concentration and melting point for the alloy for predicting hardness. Furthermore, in a recent paper, ML and atomistic simulation were combined to predict

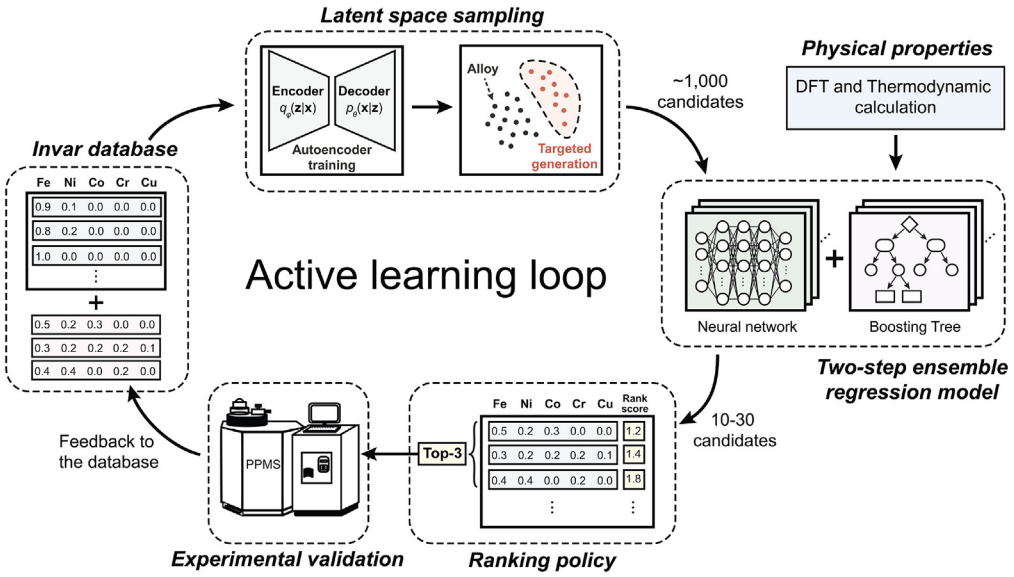

Figure 7. A schematic of active learning loop for discovery of MPEAs
Reprinted with permission from AAAS.[98]

Young's modulus and yield strength of non-equiatomic CuFeNiCrCo using 900 data points sampled by MD simulation, and the ML model was able to achieve a reasonable accuracy using only elemental compositions as the input features.[80]

As mentioned earlier, supervised learning is adopted in ML-assisted MPEA design to examine the underlying relationship between composition and property. The two types of supervised ML algorithms include classification and regression based on the targeted output variable. For classification purposes, the output is discrete and is categorized into different classes based on the labels, and a typical example is phase selection. In comparison, the output in regression is continuous, and the model makes predictions of values, such as mechanical properties, including elastic constants, hardness, yield strength, and Young's modulus. Table 1 summarizes the best-performing ML algorithms in some of the recent works, which were selected based on the predictions on testing or validation sets.

Additional strategies, such as active learning, are utilized to improve the performance of ML models.[98] In the application of MPEA discovery, newly obtained experimental data that are synthesized and measured based on the optimal candidates predicted from the previous iteration(s) can be appended to the training set. The purpose of this augmentation process is to selectively supplement near-optimum data entries in the interest of guiding the optimization route. An example of an active learning framework is illustrated in Figure 7.

From the perspective of materials science, the interpretability of ML models is also essential for gaining insights into the underlying relationship between the features and the predictions. Recent studies have started to shift their focus to this aspect. One of the strategies is to use ML models with high interpretability, such as decision trees, linear regression, and logistic regression, which might sacrifice the accuracy of the model.[99,100] Another approach is to build analytical functions fitted using ML methods and obtain the direct relation between features and output properties, as shown by Beniwal et al.[73] and Vazquez et al.[76]

MPEA design through synergistic computational methods

In this article, so far, we have discussed the contributions of various computational techniques toward the design and development of MPEA systems. End-to-end design of an alloy system warrants a combination of multiple techniques complementing each other toward the final alloy compositions and/or process parameters. Many efforts have been dedicated to the design of new MPEA systems with outstanding structural performance supported by experimental validation. Thermodynamics calculations have been used in conjunction with other atomistic methods and experiments to determine the phase stability of structural MPEAs. This has been proven to be of significant importance in designing new MPEA systems, as the stability of the random solid solution is of paramount importance.[101–104] Extensive thermodynamic databases have been developed to streamline this process. An iterative process was employed to search among more than a million alloys within the Al-Co-Cr-Cu-Fe-Ni system and progressively fabricated a total of 42 new MPEA candidates that were predicted to possess high hardness to expand the training dataset.[77] Thirty-five of the newly synthesized alloys were measured to have higher hardness values than the best ones in the original dataset, consisting of 155 samples, and the highest hardness reached 883 HV. Furthermore, a database consisting of 370 MPEAs with corresponding hardness values was adopted by Yang et al.,[78] and a novel MPEA with a hardness of 920 HV was successfully designed and validated, outperforming the top one in the original dataset by almost 25%.

Figure 8 provides a schematic representation of how the atomistic and data science methods are connected with each other and with the experimental methods toward accomplishing design goals. A constant omnidirectional flow of information can be established between these

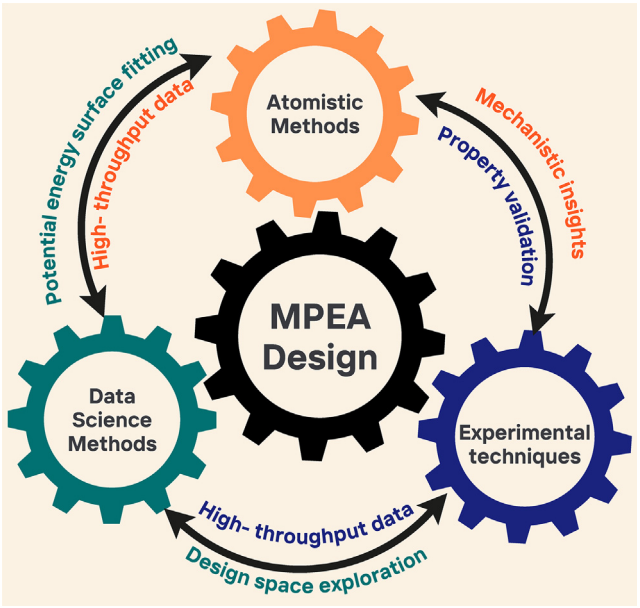

Figure 8. A schematic representation of the interconnection of different materials science paradigms toward structural MPEA design

techniques which form an integral part of not just structural MPEA design but also any material design process. Some of the challenges and future directions for these methodologies are discussed in the following section.

CHALLENGES AND PROSPECTS

Computational methods have been proven to be quintessential for the development of structural MPEAs. In the meantime, simulating MPEAs has presented complex and challenging research problems in the field. DFT calculations do not require any prior empirical data, which helps significantly in exploring the compositional space of MPEAs. Although, as the size of the system increases, the number of electrons and basis functions that must be considered also increases significantly. This poses a major challenge in the study of MPEAs as a relatively large supercell is often required to represent these systems, and they usually contain elements that have a large number of electrons. Also, the MPEA phases can be complex, including multiple phases being thermodynamically stable under the same conditions. Better integration with thermodynamic models and *ab initio* calculations can improve the reliability of the computational design process. Furthermore, to accurately model these systems, each phase must be separately modeled, and the interactions between the phases must be considered, making it extremely difficult to be simulated using DFT. Moving away from reciprocal space and exploring the possibilities of real-space DFT and other methods for accelerating the calculations such as making the sub-space diagonalization efficient can bring significant improvements to these challenges in structural MPEA research.[105–107]

Classical MD is often suggested as a viable alternative to atomistically investigating structural MPEA systems and has been used widely to study plasticity mechanisms. MD can access larger time and space scales, making it very effective in studying various phenomena. However, MD simulations require an IP and the accuracy of the simulations is significantly affected by how an IP was fitted. Classical potentials and ML-based IPs have been generated over the years for MPEAs. Existing methods, while advancing the field, have also demonstrated the complexity of the problem at hand and still need to be improved. A critical limitation on this is the ability of the current IPs to model non-equiatomic compositions of MPEAs, especially with micro-alloying. The complex phase space of the non-equiatomic MPEAs remains a challenge to model accurately using classical MD. Efforts toward developing IPs for the periodic table[108] are steps in the right direction but are still far from a reliable alternative to system-specific IPs. Structure generation for large-scale simulations is also challenging for MPEAs due to their chemical complexity and short-range ordering. Recent studies discussed in a previous section have proposed novel methods to tackle this problem and generate reliable structures with a high level of confidence.[21,22] Still, there is a significant disconnect within the structure generation algorithms while considering the thermodynamic stability of the structures that need to be addressed.

The recent progress in ML-aided MPEA design for structural applications has been discussed from four aspects, the output properties, material database, descriptors, and ML algorithms. Despite the enormous work devoted to this field, three major challenges remain. First, a reliable and well-structured MPEA database for mechanical properties, which is essential for improving the quality of ML tools, is absent. A recently compiled MPEA database published by Citrine Informatics contains experimentally measured mechanical properties of 630 compositions,[87] but the reported properties vary significantly with the fabrication and characterization techniques. Comparative analysis and generalization of data continue to be challenging with MPEAs due to different synthesizing techniques, testing conditions, and phase complexities.[87] A comprehensive computational database would be relevant in this context for MPEA systems. Second, the descriptors selected for ML models differ significantly even for the same output properties, indicating that the underlying relationship between composition and

property has not been unrevealed, and a more decent feature selection method is needed. Lastly, most of the outcomes retrieved from ML approaches have poor interpretability, and the contribution to new materials science knowledge is limited.

SUPPLEMENTAL INFORMATION

Supplemental information can be found online at https://doi.org/10.1016/j.isci.2023.107751.

ACKNOWLEDGMENTS

Financial support for this work was provided through the Natural Sciences and Engineering Research Council of Canada (NSERC) and Early Researcher Award from the province of Ontario, Canada.

AUTHOR CONTRIBUTIONS

A.A.: Conceptualization, Investigation, Writing-original draft. S.L.: Conceptualization, Investigation, Writing-original draft. C.V.S.: Supervision, Review and Editing.

DECLARATION OF INTERESTS

The authors declare no competing interests.

REFERENCES

1. Senkov, O.N., Miller, J.D., Miracle, D.B., and Woodward, C. (2015). Accelerated exploration of multi-principal element alloys with solid solution phases. Nat. Commun. *6*, 1–10. https://doi.org/10.1038/ncomms7529.
2. Pickering, E.J., and Jones, N.G. (2016). High-entropy alloys: a critical assessment of their founding principles and future prospects. Int. Mater. Rev. *61*, 183–202. https://doi.org/10.1080/09506608.2016.1180020.
3. Senkov, O.N., and Semiatin, S.L. (2015). Microstructure and properties of a refractory high-entropy alloy after cold working. J. Alloys Compd. *649*, 1110–1123. https://doi.org/10.1016/J.JALLCOM.2015.07.209.
4. Miracle, D.B., and Senkov, O.N. (2017). A critical review of high entropy alloys and related concepts. Acta Mater. *122*, 448–511. https://doi.org/10.1016/J.ACTAMAT.2016.08.081.
5. George, E.P., Raabe, D., and Ritchie, R.O. (2019). High-entropy alloys. Nat. Rev. Mater. *4*, 515–534. https://doi.org/10.1038/S41578-019-0121-4.
6. Gludovatz, B., Hohenwarter, A., Catoor, D., Chang, E.H., George, E.P., and Ritchie, R.O. (2014). A fracture-resistant high-entropy alloy for cryogenic applications. Science *345*, 1153–1158. https://doi.org/10.1126/SCIENCE.1254581/SUPPL_FILE/GLUDOVATZ.SM.PDF.
7. Li, Z., Zhao, S., Ritchie, R.O., and Meyers, M.A. (2019). Mechanical properties of high-entropy alloys with emphasis on face-centered cubic alloys. Prog. Mater. Sci. *102*, 296–345. https://doi.org/10.1016/J.PMATSCI.2018.12.003.
8. Li, W., Xie, D., Li, D., Zhang, Y., Gao, Y., and Liaw, P.K. (2021). Mechanical behavior of high-entropy alloys. Prog. Mater. Sci. *118*, 100777. https://doi.org/10.1016/J.PMATSCI.2021.100777.
9. Miao, J., Guo, T., Ren, J., Zhang, A., Su, B., and Meng, J. (2018). Optimization of mechanical and tribological properties of FCC CrCoNi multi-principal element alloy with Mo addition. Vacuum *149*, 324–330. https://doi.org/10.1016/J.VACUUM.2018.01.012.
10. Deng, G., Tieu, A.K., Su, L., Wang, P., Wang, L., Lan, X., Cui, S., and Zhu, H. (2020). Investigation into reciprocating dry sliding friction and wear properties of bulk CoCrFeNiMo high entropy alloys fabricated by spark plasma sintering and subsequent cold rolling processes: Role of Mo element concentration. Wear *460–461*, 203440. https://doi.org/10.1016/J.WEAR.2020.203440.
11. Zhai, W., Bai, L., Zhou, R., Fan, X., Kang, G., Liu, Y., and Zhou, K. (2021). Recent Progress on Wear-Resistant Materials: Designs, Properties, and Applications. Adv. Sci. *8*, 2003739. https://doi.org/10.1002/ADVS.202003739.
12. Lee, D.H., Seok, M.Y., Zhao, Y., Choi, I.C., He, J., Lu, Z., Suh, J.Y., Ramamurty, U., Kawasaki, M., Langdon, T.G., and Jang, J.i. (2016). Spherical nanoindentation creep behavior of nanocrystalline and coarse-grained CoCrFeMnNi high-entropy alloys. Acta Mater. *109*, 314–322. https://doi.org/10.1016/J.ACTAMAT.2016.02.049.
13. Vaidya, M., Trubel, S., Murty, B.S., Wilde, G., and Divinski, S.v. (2016). Ni tracer diffusion in CoCrFeNi and CoCrFeMnNi high entropy alloys. J. Alloys Compd. *688*, 994–1001. https://doi.org/10.1016/J.JALLCOM.2016.07.239.
14. Hemphill, M.A., Yuan, T., Wang, G.Y., Yeh, J.W., Tsai, C.W., Chuang, A., and Liaw, P.K. (2012). Fatigue behavior of Al0.5CoCrCuFeNi high entropy alloys. Acta Mater. *60*, 5723–5734. https://doi.org/10.1016/J.ACTAMAT.2012.06.046.
15. Zhang, Y., Zuo, T.T., Tang, Z., Gao, M.C., Dahmen, K.A., Liaw, P.K., and Lu, Z.P. (2014). Microstructures and properties of high-entropy alloys. Prog. Mater. Sci. *61*, 1–93. https://doi.org/10.1016/J.PMATSCI.2013.10.001.
16. Tsai, M.H., and Yeh, J.W. (2014). High-Entropy Alloys: A Critical Review. *2*, 107–123. https://doi.org/10.1080/21663831.2014.912690. http://mc.manuscriptcentral.com/tmrl.
17. Ångqvist, M., Muñoz, W.A., Rahm, J.M., Fransson, E., Durniak, C., Rozyczko, P., Rod, T.H., and Erhart, P. (2019). ICET – A Python library for constructing and sampling alloy cluster expansions. Adv. Theory Simul. *2*, 1900015. https://doi.org/10.1002/adts.201900015.
18. Van De Walle, A., Tiwary, P., De Jong, M., Olmsted, D.L., Asta, M., Dick, A., Shin, D., Wang, Y., Chen, L.Q., and Liu, Z.K. (2013). Efficient stochastic generation of special quasirandom structures. Calphad *42*, 13–18. https://doi.org/10.1016/j.calphad.2013.06.006.
19. Van de Walle, A., Asta, M., and Ceder, G. (2002). The alloy theoretic automated toolkit: A user guide. Calphad *26*, 539–553. https://doi.org/10.1016/S0364-5916(02)80006-2.
20. Okhotnikov, K., Charpentier, T., and Cadars, S. (2016). Supercell program: A combinatorial structure-generation approach for the local-level modeling of atomic substitutions and partial occupancies in crystals. J. Cheminform. *8*, 17. https://doi.org/10.1186/S13321-016-0129-3/FIGURES/4.
21. Tetsassi Feugmo, C.G., Ryczko, K., Anand, A., Singh, C.V., and Tamblyn, I. (2021). Neural evolution structure generation: High entropy alloys. J. Chem. Phys. *155*, 044102. https://doi.org/10.1063/5.0049000.
22. Fey, L.T.W., and Beyerlein, I.J. (2022). Random Generation of Lattice Structures with Short-Range Order. Integr. Mater. Manuf. Innov. *11*, 382–390. https://doi.org/10.1007/S40192-022-00269-0/TABLES/1.
23. Oh, H.S., Odbadrakh, K., Ikeda, Y., Mu, S., Körmann, F., Sun, C.J., Ahn, H.S., Yoon, K.N., Ma, D., Tasan, C.C., et al. (2021). Element-resolved local lattice distortion in complex concentrated alloys: An observable signature of electronic effects. Acta Mater. *216*, 117135. https://doi.org/10.1016/J.ACTAMAT.2021.117135.
24. Ishibashi, S., Ikeda, Y., Körmann, F., Grabowski, B., and Neugebauer, J. (2020). Correlation analysis of strongly fluctuating atomic volumes, charges, and stresses in body-centered cubic refractory high-entropy alloys. Phys. Rev. Mater. *4*, 023608. https://doi.org/10.1103/

PHYSREVMATERIALS.4.023608/FIGURES/7/MEDIUM.
25. Tong, Y., Zhao, S., Bei, H., Egami, T., Zhang, Y., and Zhang, F. (2020). Severe local lattice distortion in Zr- and/or Hf-containing refractory multi-principal element alloys. Acta Mater. *183*, 172–181. https://doi.org/10.1016/J.ACTAMAT.2019.11.026.
26. Okamoto, N.L., Yuge, K., Tanaka, K., Inui, H., and George, E.P. (2016). Atomic displacement in the CrMnFeCoNi high-entropy alloy – A scaling factor to predict solid solution strengthening. AIP Adv. *6*, 125008. https://doi.org/10.1063/1.4971371.
27. Oh, H., Ma, D., Leyson, G., Grabowski, B., Park, E., Körmann, F., and Raabe, D. (2016). Lattice Distortions in the FeCoNiCrMn High Entropy Alloy Studied by Theory and Experiment. Entropy *18*, 321. https://doi.org/10.3390/E18090321.
28. Sohn, S.S., Kwiatkowski da Silva, A., Ikeda, Y., Körmann, F., Lu, W., Choi, W.S., Gault, B., Ponge, D., Neugebauer, J., and Raabe, D. (2019). Ultrastrong Medium-Entropy Single-Phase Alloys Designed via Severe Lattice Distortion. Adv. Mater. *31*, 1807142. https://doi.org/10.1002/ADMA.201807142.
29. Oh, H.S., Kim, S.J., Odbadrakh, K., Ryu, W.H., Yoon, K.N., Mu, S., Körmann, F., Ikeda, Y., Tasan, C.C., Raabe, D., et al. (2019). Engineering atomic-level complexity in high-entropy and complex concentrated alloys. Nat. Commun. *10*, 2090. https://doi.org/10.1038/s41467-019-10012-7.
30. Singh, P., Smirnov, A.V., Alam, A., and Johnson, D.D. (2020). First-principles prediction of incipient order in arbitrary high-entropy alloys: exemplified in Ti0.25CrFeNiAlx. Acta Mater. *189*, 248–254. https://doi.org/10.1016/J.ACTAMAT.2020.02.063.
31. Zhang, B., Ding, J., and Ma, E. (2021). Chemical short-range order in body-centered-cubic TiZrHfNb high-entropy alloys. Appl. Phys. Lett. *119*, 201908. https://doi.org/10.1063/5.0069417.
32. Singh, P., Gupta, S., Thimmaiah, S., Thoeny, B., Ray, P.K., Smirnov, A.V., Johnson, D.D., and Kramer, M.J. (2020). Vacancy-mediated complex phase selection in high entropy alloys. Acta Mater. *194*, 540–546. https://doi.org/10.1016/J.ACTAMAT.2020.04.063.
33. Yin, B., and Curtin, W.A. (2019). First-principles-based prediction of yield strength in the RhIrPdPtNiCu high-entropy alloy. npj Comput. Mater. *5*, 14–17. https://doi.org/10.1038/s41524-019-0151-x.
34. Chen, B., Li, S., Zong, H., Ding, X., Sun, J., and Ma, E. (2020). Unusual activated processes controlling dislocation motion in body-centered-cubic high-entropy alloys. Proc Natl Acad Sci USA *117*, 16199–16206. https://doi.org/10.1073/PNAS.1919136117/SUPPL_FILE/PNAS.1919136117.SM02.MP4.
35. Wang, F., Balbus, G.H., Xu, S., Su, Y., Shin, J., Rottmann, P.F., Knipling, K.E., Stinville, J.C., Mills, L.H., Senkov, O.N., et al. (2020). Multiplicity of dislocation pathways in a refractory multiprincipal element alloy. Science *370*, 95–101. https://doi.org/10.1126/SCIENCE.ABA3722/SUPPL_FILE/ABA3722_WANG_SM.PDF.
36. Xu, S., Su, Y., Jian, W.R., and Beyerlein, I.J. (2021). Local slip resistances in equal-molar MoNbTi multi-principal element alloy. Acta Mater. *202*, 68–79. https://doi.org/10.1016/J.ACTAMAT.2020.10.042.
37. Romero, R.A., Xu, S., Jian, W.R., Beyerlein, I.J., and Ramana, C.V. (2022). Atomistic simulations of the local slip resistances in four refractory multi-principal element alloys. Int. J. Plast. *149*, 103157. https://doi.org/10.1016/J.IJPLAS.2021.103157.
38. Varvenne, C., and Curtin, W.A. (2017). Strengthening of high entropy alloys by dilute solute additions: CoCrFeNiAl and CoCrFeNiMnAl alloys. Scr. Mater. *138*, 92–95. https://doi.org/10.1016/j.scriptamat.2017.05.035.
39. Yeh, J.W., Chen, S.K., Lin, S.J., Gan, J.Y., Chin, T.S., Shun, T.T., Tsau, C.H., and Chang, S.Y. (2004). Nanostructured high-entropy alloys with multiple principal elements: novel alloy design concepts and outcomes. Adv. Eng. Mater. *6*, 299–303. https://doi.org/10.1002/adem.200300567.
40. Yan, J., Yin, S., Asta, M., Ritchie, R.O., Ding, J., and Yu, Q. (2022). Anomalous size effect on yield strength enabled by compositional heterogeneity in high-entropy alloy nanoparticles. Nat. Commun. *13*, 2789. https://doi.org/10.1038/s41467-022-30524-z.
41. Jin, K., Lu, C., Wang, L.M., Qu, J., Weber, W.J., Zhang, Y., and Bei, H. (2016). Effects of compositional complexity on the ion-irradiation induced swelling and hardening in Ni-containing equiatomic alloys. Scr. Mater. *119*, 65–70. https://doi.org/10.1016/J.SCRIPTAMAT.2016.03.030.
42. Zhang, Y., Wang, Y., Yan, Z., Song, C., Miao, G., and Zhang, L. (2019). Dissipation of radiation energy in concentrated solid-solution alloys: Unique defect properties and microstructural evolution. MRS Bull. *24*, 798–811. https://doi.org/10.1557/MRS.2019.233.
43. Zhang, Y., Stocks, G.M., Jin, K., Lu, C., Bei, H., Sales, B.C., Wang, L., Béland, L.K., Stoller, R.E., Samolyuk, G.D., et al. (2015). Influence of chemical disorder on energy dissipation and defect evolution in concentrated solid solution alloys. Nat. Commun. *6*, 1–9. https://doi.org/10.1038/ncomms9736.
44. Zhang, Y., Zhou, H., Perkins, A., Wang, Y., Sun, J., and Djurabekova, F. (2017). Atomic-level heterogeneity and defect dynamics in concentrated solid-solution alloys. Nutrients *9*, 221–237. https://doi.org/10.1016/J.COSSMS.2017.02.002.
45. Qian, L., Bao, H., Li, R., and Peng, Q. (2022). Atomistic insights of a chemical complexity effect on the irradiation resistance of high entropy alloys. Mater. Adv. *3*, 1680–1686. https://doi.org/10.1039/D1MA01184G.
46. Deluigi, O.R., Pasianot, R.C., Valencia, F.J., Caro, A., Farkas, D., and Bringa, E.M. (2021). Simulations of primary damage in a High Entropy Alloy: Probing enhanced radiation resistance. Acta Mater. *213*, 116951. https://doi.org/10.1016/J.ACTAMAT.2021.116951.
47. Lin, Y., Yang, T., Lang, L., Shan, C., Deng, H., Hu, W., and Gao, F. (2020). Enhanced radiation tolerance of the Ni-Co-Cr-Fe high-entropy alloy as revealed from primary damage. Acta Mater. *196*, 133–143. https://doi.org/10.1016/J.ACTAMAT.2020.06.027.
48. Tuomisto, F., Makkonen, I., Heikinheimo, J., Granberg, F., Djurabekova, F., Nordlund, K., Velisa, G., Bei, H., Xue, H., Weber, W.J., and Zhang, Y. (2020). Segregation of Ni at early stages of radiation damage in NiCoFeCr solid solution alloys. Acta Mater. *196*, 44–51. https://doi.org/10.1016/J.ACTAMAT.2020.06.024.
49. Xu, Q., Guan, H.Q., Zhong, Z.H., Huang, S.S., and Zhao, J.J. (2021). Irradiation resistance mechanism of the CoCrFeMnNi equiatomic high-entropy alloy. Sci. Rep. *11*, 608. https://doi.org/10.1038/s41598-020-79775-0.
50. Lach, T.G., Silva, C.M., Zhou, Y., Boldman, W.L., Rack, P.D., Weber, W.J., and Zhang, Y. (2022). Dynamic substrate reactions during room temperature heavy ion irradiation of CoCrCuFeNi high entropy alloy thin films. npj Mater. Degrad. *6*. 60–15. https://doi.org/10.1038/s41529-022-00260-2.
51. Peng, J., Xie, B., Zeng, X., Fang, Q., Liu, B., Liaw, P.K., and Li, J. (2022). Vacancy dependent mechanical behaviors of high-entropy alloy. Int. J. Mech. Sci. *218*, 107065. https://doi.org/10.1016/J.IJMECSCI.2022.107065.
52. Zhang, Z., Su, Z., Zhang, B., Yu, Q., Ding, J., Shi, T., Lu, C., Ritchie, R.O., and Ma, E. (2023). Effect of local chemical order on the irradiation-induced defect evolution in CrCoNi medium-entropy alloy. Proc Natl Acad Sci USA *120*, e2218673120. https://doi.org/10.1073/PNAS.2218673120/SUPPL_FILE/PNAS.2218673120.SAPP.PDF.
53. Farkas, D., and Caro, A. (2020). Model interatomic potentials for Fe-Ni-Cr-Co-Al high-entropy alloys. J. Mater. Res. *35*, 3031–3040. https://doi.org/10.1557/JMR.2020.294/METRICS.
54. Gröger, R., Vitek, V., and Dlouhý, A. (2020). Effective pair potential for random fcc CoCrFeMnNi alloys. Model. Simul. Mat. Sci. Eng. *28*, 075006. https://doi.org/10.1088/1361-651X/AB7F8B.
55. Shapeev, A.V. (2016). Moment Tensor Potentials: A Class of Systematically Improvable Interatomic Potentials, pp. 1153–1173. https://doi.org/10.1137/15M1054183.
56. Nyshadham, C., Rupp, M., Bekker, B., Shapeev, A.V., Mueller, T., Rosenbrock, C.W., Csányi, G., Wingate, D.W., and Hart, G.L.W. (2019). Machine-learned multi-system surrogate models for materials prediction. npj Comput. Mater. *5*, 51–56. https://doi.org/10.1038/s41524-019-0189-9.
57. Grabowski, B., Ikeda, Y., Srinivasan, P., Körmann, F., Freysoldt, C., Duff, A.I., Shapeev, A., and Neugebauer, J. (2019). Ab initio vibrational free energies including anharmonicity for multicomponent alloys. npj Comput. Mater. *5*, 80–86. https://doi.org/10.1038/s41524-019-0218-8.
58. Jafary-Zadeh, M., Khoo, K.H., Laskowski, R., Branicio, P.S., and Shapeev, A.V. (2019). Applying a machine learning interatomic potential to unravel the effects of local lattice distortion on the elastic properties of multi-principal element alloys. J. Alloys Compd. *803*, 1054–1062. https://doi.org/10.1016/J.JALLCOM.2019.06.318.
59. Novikov, I.S., Gubaev, K., Podryabinkin, E.V., Shapeev, A.V., Long, T., Novikov, I.S., Gubaev, K., Podryabinkin, E.V., and Shapeev, A.V. (2021). The MLIP package: moment tensor potentials with MPI and active learning. Mach Learn Sci Technol *2*, 025002. https://doi.org/10.1088/2632-2153/ABC9FE.
60. Yin, S., Zuo, Y., Abu-Odeh, A., Zheng, H., Li, X.G., Ding, J., Ong, S.P., Asta, M., and Ritchie, R.O. (2021). Atomistic simulations of dislocation mobility in refractory high-entropy alloys and the effect of chemical short-range order. Nat. Commun. *12*, 4873. https://doi.org/10.1038/s41467-021-25134-0.

61. Zhou, Y., Srinivasan, P., Körmann, F., Grabowski, B., Smith, R., Goddard, P., and Duff, A.I. (2022). Thermodynamics up to the melting point in a TaVCrW high entropy alloy: Systematic ab initio study aided by machine learning potentials. Phys. Rev. B *105*, 214302. https://doi.org/10.1103/PHYSREVB.105.214302/FIGURES/9/MEDIUM.
62. Shapeev, A. (2017). Accurate representation of formation energies of crystalline alloys with many components. Comput. Mater. Sci. *139*, 26–30. https://doi.org/10.1016/J.COMMATSCI.2017.07.010.
63. Kostiuchenko, T., Körmann, F., Neugebauer, J., and Shapeev, A. (2019). Impact of lattice relaxations on phase transitions in a high-entropy alloy studied by machine-learning potentials. npj Comput. Mater. *5*, 1–7. https://doi.org/10.1038/s41524-019-0195-y.
64. Meshkov, E.A., Novoselov, I.I., Shapeev, A.V., and Yanilkin, A.V. (2019). Sublattice formation in CoCrFeNi high-entropy alloy. Intermetallics *112*, 106542. https://doi.org/10.1016/J.INTERMET.2019.106542.
65. Deringer, V.L., Bartók, A.P., Bernstein, N., Wilkins, D.M., Ceriotti, M., and Csányi, G. (2021). Gaussian Process Regression for Materials and Molecules. Chem Rev *121*, 10073–10141. https://doi.org/10.1021/ACS.CHEMREV.1C00022/ASSET/IMAGES/MEDIUM/CR1C00022_M069.GIF.
66. Dhaliwal, G., Nair, P.B., and Singh, C.V. (2022). Machine learned interatomic potentials using random features. npj Comput. Mater. *8*, 1–10. https://doi.org/10.1038/s41524-021-00685-4.
67. Dhaliwal, G., Anand, A., Nair, P.B., and Singh, C.V. (2023). Sparse Random Fourier Features Based Interatomic Potentials for High Entropy Alloys. https://doi.org/10.48550/arxiv.2302.06844.
68. Li, X.G., Chen, C., Zheng, H., Zuo, Y., and Ong, S.P. (2020). Complex strengthening mechanisms in the NbMoTaW multi-principal element alloy. npj Comput. Mater. *6*, 1–10. https://doi.org/10.1038/s41524-020-0339-0.
69. Thompson, A.P., Swiler, L.P., Trott, C.R., Foiles, S.M., and Tucker, G.J. (2015). Spectral neighbor analysis method for automated generation of quantum-accurate interatomic potentials. J. Comput. Phys. *285*, 316–330. https://doi.org/10.1016/J.JCP.2014.12.018.
70. Bartók, A.P., Payne, M.C., Kondor, R., and Csányi, G. (2010). Gaussian approximation potentials: The accuracy of quantum mechanics, without the electrons. Phys. Rev. Lett. *104*, 136403. https://doi.org/10.1103/PHYSREVLETT.104.136403/FIGURES/4/MEDIUM.
71. Pei, Z., Yin, J., Hawk, J.A., Alman, D.E., and Gao, M.C. (2020). Machine-learning informed prediction of high-entropy solid solution formation: Beyond the Hume-Rothery rules. npj Comput. Mater. *6*, 50–58. https://doi.org/10.1038/s41524-020-0308-7.
72. Beniwal, D., and Ray, P.K. (2021). Learning phase selection and assemblages in High-Entropy Alloys through a stochastic ensemble-averaging model. Comput. Mater. Sci. *197*, 110647. https://doi.org/10.1016/J.COMMATSCI.2021.110647.
73. Beniwal, D., and Ray, P.K. (2022). FCC vs. BCC phase selection in high-entropy alloys via simplified and interpretable reduction of machine learning models. Materialia (Oxf) *26*, 101632. https://doi.org/10.1016/J.MTLA.2022.101632.
74. Revi, V., Kasodariya, S., Talapatra, A., Pilania, G., and Alankar, A. (2021). Machine learning elastic constants of multi-component alloys. Comput. Mater. Sci. *198*, 110671. https://doi.org/10.1016/J.COMMATSCI.2021.110671.
75. Bhandari, U., Ghadimi, H., Zhang, C., Yang, S., and Guo, S. (2022). Predicting Elastic Constants of Refractory Complex Concentrated Alloys Using Machine Learning Approach. Materials *15*, 4997. https://doi.org/10.3390/MA15144997.
76. Vazquez, G., Singh, P., Sauceda, D., Couperthwaite, R., Britt, N., Youssef, K., Johnson, D.D., and Arróyave, R. (2022). Efficient machine-learning model for fast assessment of elastic properties of high-entropy alloys. Acta Mater. *232*, 117924. https://doi.org/10.1016/J.ACTAMAT.2022.117924.
77. Wen, C., Zhang, Y., Wang, C., Xue, D., Bai, Y., Antonov, S., Dai, L., Lookman, T., and Su, Y. (2019). Machine learning assisted design of high entropy alloys with desired property. Acta Mater. *170*, 109–117. https://doi.org/10.1016/J.ACTAMAT.2019.03.010.
78. Yang, C., Ren, C., Jia, Y., Wang, G., Li, M., and Lu, W. (2022). A machine learning-based alloy design system to facilitate the rational design of high entropy alloys with enhanced hardness. Acta Mater. *222*, 117431. https://doi.org/10.1016/J.ACTAMAT.2021.117431.
79. Zhang, L., Qian, K., Huang, J., Liu, M., and Shibuta, Y. (2021). Molecular dynamics simulation and machine learning of mechanical response in non-equiatomic FeCrNiCoMn high-entropy alloy. J. Mater. Res. Technol. *13*, 2043–2054. https://doi.org/10.1016/J.JMRT.2021.06.021.
80. Zhang, L., Qian, K., Schuller, B.W., and Shibuta, Y. (2021). Prediction on mechanical properties of non-equiatomic high-entropy alloy by atomistic simulation and machine learning. Metals *11*, 922. https://doi.org/10.3390/MET11060922/S1.
81. Khakurel, H., Taufique, M.F.N., Roy, A., Balasubramanian, G., Ouyang, G., Cui, J., Johnson, D.D., and Devanathan, R. (2021). Machine learning assisted prediction of the Young's modulus of compositionally complex alloys. Sci. Rep. *11*, 17149. https://doi.org/10.1038/s41598-021-96507-0.
82. Gao, Y., Bai, S., Chong, K., Liu, C., Cao, Y., and Zou, Y. (2023). Machine learning accelerated design of non-equiatomic refractory high entropy alloys based on first principles calculation. Vacuum *207*, 111608. https://doi.org/10.1016/J.VACUUM.2022.111608.
83. Sun, S.J., Tian, Y.Z., Lin, H.R., Yang, H.J., Dong, X.G., Wang, Y.H., and Zhang, Z.F. (2019). Achieving high ductility in the 1.7 GPa grade CoCrFeMnNi high-entropy alloy at 77 K. Materials Science and Engineering: A *740–741*, 336–341. https://doi.org/10.1016/J.MSEA.2018.10.094.
84. Tian, Y.Z., Sun, S.J., Lin, H.R., and Zhang, Z.F. (2019). Fatigue behavior of CoCrFeMnNi high-entropy alloy under fully reversed cyclic deformation. J. Mater. Sci. Technol. *35*, 334–340. https://doi.org/10.1016/J.JMST.2018.09.068.
85. Guo, L., Ou, X., Ni, S., Liu, Y., and Song, M. (2019). Effects of carbon on the microstructures and mechanical properties of FeCoCrNiMn high entropy alloys. Materials Science and Engineering: A *746*, 356–362. https://doi.org/10.1016/J.MSEA.2019.01.050.
86. Gao, M.C., Zhang, C., Gao, P., Zhang, F., Ouyang, L.Z., Widom, M., and Hawk, J.A. (2017). Thermodynamics of concentrated solid solution alloys. Curr. Opin. Solid State Mater. Sci. *21*, 238–251. https://doi.org/10.1016/J.COSSMS.2017.08.001.
87. Borg, C.K.H., Frey, C., Moh, J., Pollock, T.M., Gorsse, S., Miracle, D.B., Senkov, O.N., Meredig, B., and Saal, J.E. (2020). Expanded dataset of mechanical properties and observed phases of multi-principal element alloys. Sci. Data *7*, 430–436. https://doi.org/10.1038/s41597-020-00768-9.
88. Couzinié, J.P., Senkov, O.N., Miracle, D.B., and Dirras, G. (2018). Comprehensive data compilation on the mechanical properties of refractory high-entropy alloys. Data Brief *21*, 1622–1641. https://doi.org/10.1016/J.DIB.2018.10.071.
89. Gorsse, S., Nguyen, M.H., Senkov, O.N., and Miracle, D.B. (2018). Database on the mechanical properties of high entropy alloys and complex concentrated alloys. Data Brief *21*, 2664–2678. https://doi.org/10.1016/J.DIB.2018.11.111.
90. Roy, A., and Balasubramanian, G. (2021). Predictive descriptors in machine learning and data-enabled explorations of high-entropy alloys. Comput. Mater. Sci. *193*, 110381. https://doi.org/10.1016/j.commatsci.2021.110381.
91. Huang, W., Martin, P., and Zhuang, H.L. (2019). Machine-learning phase prediction of high-entropy alloys. Acta Mater. *169*, 225–236. https://doi.org/10.1016/J.ACTAMAT.2019.03.012.
92. Zhou, Z., Zhou, Y., He, Q., Ding, Z., Li, F., and Yang, Y. (2019). Machine learning guided appraisal and exploration of phase design for high entropy alloys. NPJ Comput. Mater. *5*, 128. https://doi.org/10.1038/s41524-019-0265-1.
93. Zhang, Y., Lu, Y., Wang, L., Tian, Y., Zhang, Z., Bai, Y., and Su, Y. (2020). Phase prediction in high entropy alloys with a rational selection of materials descriptors and machine learning models. Drug Res. *70*, 528–540. https://doi.org/10.1016/J.ACTAMAT.2019.11.067.
94. Krishna, Y.V., Jaiswal, U.K., and Rahul, R.M. (2021). Machine learning approach to predict new multiphase high entropy alloys. Scr. Mater. *197*, 113804. https://doi.org/10.1016/J.SCRIPTAMAT.2021.113804.
95. Risal, S., Zhu, W., Guillen, P., and Sun, L. (2021). Improving phase prediction accuracy for high entropy alloys with Machine learning. Comput. Mater. Sci. *192*, 110389. https://doi.org/10.1016/J.COMMATSCI.2021.110389.
96. Zhao, D.Q., Pan, S.P., Zhang, Y., Liaw, P.K., and Qiao, J.W. (2021). Structure prediction in high-entropy alloys with machine learning. Appl. Phys. Lett. *118*. https://doi.org/10.1063/5.0051307.
97. King, D.J.M., Middleburgh, S.C., McGregor, A.G., and Cortie, M.B. (2016). Predicting the formation and stability of single phase high-entropy alloys. Acta Mater. *104*, 172–179. https://doi.org/10.1016/J.ACTAMAT.2015.11.040.
98. Rao, Z., Tung, P.Y., Xie, R., Wei, Y., Zhang, H., Ferrari, A., Klaver, T.P.C., Körmann, F., Sukumar, P.T., da Silva, A.K., et al. (2022). Machine learning–enabled high-entropy alloy discovery. Science *378*, 78–85. https://

doi.org/10.1126/SCIENCE.ABO4940/SUPPL_FILE/SCIENCE.ABO4940_SM.PDF.

99. Pintelas, E., Livieris, I.E., and Pintelas, P. (2020). A Grey-Box Ensemble Model Exploiting Black-Box Accuracy and White-Box Intrinsic Interpretability. Algorithms *13*, 17. https://doi.org/10.3390/A13010017.
100. Linardatos, P., Papastefanopoulos, V., and Kotsiantis, S. (2020). Explainable AI: A Review of Machine Learning Interpretability Methods. Entropy *23*, 18–45. https://doi.org/10.3390/E23010018.
101. Chung, D.H., Kim, W.C., Baek, S.Y., Kim, M.H., and Na, Y.S. (2022). Thermodynamics-based design strategy for optimizing strength and ductility of Cr-Ni-Mn-Fe medium-entropy alloys. J. Alloys Compd. *899*, 163331. https://doi.org/10.1016/J.JALLCOM.2021.163331.
102. Liu, Y., Liu, W., Zhou, Q.Y., Liu, C., Fan, T.W., Wu, Y.Z., Wang, Z.P., and Tang, P.Y. (2022). An initio study of thermodynamic and fracture properties of CrFeCoNiMnx ($0 \leq x \leq 3$) high-entropy alloys. J. Mater. Res. Technol. *17*, 498–506. https://doi.org/10.1016/J.JMRT.2022.01.013.
103. Biermair, F., Razumovskiy, V.I., and Ressel, G. (2022). Influence of alloying on thermodynamic properties of AlCoCrFeNiTi high entropy alloys from DFT calculations. Comput. Mater. Sci. *202*, 110952. https://doi.org/10.1016/J.COMMATSCI.2021.110952.
104. He, T., Chen, X., Qi, Y., and Feng, M. (2022). Phase-field simulation of phase separation coupled with thermodynamic databases in FeNiCrCoCu high-entropy alloys. Appl. Phys. A *128*, 987. https://doi.org/10.1007/S00339-022-06101-Y.
105. Nakata, A., Baker, J.S., Mujahed, S.Y., Poulton, J.T.L., Arapan, S., Lin, J., Raza, Z., Yadav, S., Truflandier, L., Miyazaki, T., and Bowler, D.R. (2020). Large scale and linear scaling DFT with the CONQUEST code. J. Chem. Phys. *152*, 164112. https://doi.org/10.1063/5.0005074/198783.
106. Michaud-Rioux, V., Zhang, L., and Guo, H. (2016). RESCU: A real space electronic structure method. J. Comput. Phys. *307*, 593–613. https://doi.org/10.1016/J.JCP.2015.12.014.
107. Ratcliff, L.E., Dawson, W., Fisicaro, G., Caliste, D., Mohr, S., Degomme, A., Videau, B., Cristiglio, V., Stella, M., D'Alessandro, M., et al. (2020). Flexibilities of wavelets as a computational basis set for large-scale electronic structure calculations. J. Chem. Phys. *152*, 194110. https://doi.org/10.1063/5.0004792/199040.
108. Chen, C., and Ong, S.P. (2022). A universal graph deep learning interatomic potential for the periodic table. Nat. Comput. Sci. *2*, 718–728. https://doi.org/10.1038/s43588-022-00349-3.